NANO LETTERS

pubs.acs.org/NanoLett Letter

Ultrafast Optical Modulation of Harmonic Generation in Two-Dimensional Materials

Yang Cheng,[†] Hao Hong,[†] Hui Zhao,[†] Chunchun Wu, Yu Pan, Can Liu, Yonggang Zuo, Zhihong Zhang, Jin Xie, Jinhuan Wang, Dapeng Yu, Yu Ye, Sheng Meng, and Kaihui Liu*

Cite This: *Nano Lett.* 2020, 20, 8053−8058 Read Online

ACCESS | Metrics & More | Article Recommendations | Supporting Information

ABSTRACT: The modulation of optical harmonic generation in two-dimensional (2D) materials is of paramount importance in nanophotonic and nano-optoelectronic devices for their applications in optical switching and communication. However, an effective route with ultrafast modulation speed, ultrahigh modulation depth, and broad operation wavelength range is awaiting a full exploration. Here, we report that an optical pump can dynamically modulate the third harmonic generation (THG) of a graphene monolayer with a relative modulation depth above 90% at a time scale of 2.5 ps for a broad frequency ranging from near-infrared to ultraviolet. Our observation, together with the real-time, time-dependent density functional theory (TDDFT) simulations, reveals that this modulation process stems from nonlinear dynamics of the photoexcited carriers in graphene. The superior performance of the nonlinear all-optical modulator based on 2D materials paves the way for its potential applications including nanolasers and optical communication circuits.

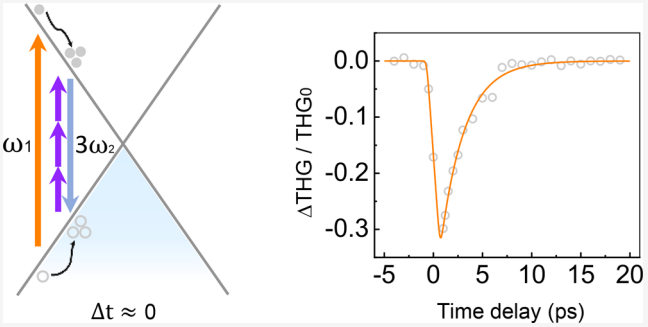

KEYWORDS: *two-dimensional materials, nonlinear optics, time-resolved THG, real-time TDDFT simulations*

Graphene is a model 2D material for investigating novel physics and applications in nanophotonics and nano-optoelectronics.[1−3] The unique linear and gapless 2D band structure that hosts massless Dirac Fermions endows graphene with strong light−matter interaction in both linear and nonlinear regimes.[4] With a light−matter interaction length of only ∼0.33 nm, the linear absorbance of graphene monolayer holds a constant coefficient of 2.3% in a wide spectrum ranging from terahertz to ultraviolet.[5,6] Although graphene is nearly transparent in the linear optical regime, the Dirac Fermions that promise enhanced electronic correlations and resonant excitation in nature give rise to large nonlinear transition dipole matrix elements and extremely strong optical nonlinearities. As a result, its third-order susceptibility that is responsible for THG and four-wave mixing is reported to be several orders of magnitude larger than that of other transparent materials.[7−9] Moreover, processes of saturable absorption,[10,11] optical bistability,[12,13] high-harmonic generation,[14−16] etc., are all observed to be highly efficient in graphene monolayer. Recently, the three-dimensional bulk materials accommodating the Dirac Fermions that possess efficient generation of high harmonic radiation should also be an important future direction.[17,18]

The modulation of optical properties lays the foundation of realizing many applications including optical switching, interconnects, and communication. Previously, enormous mechanisms, such as electro-optic, thermo-optic, magneto-optic, and acousto-optic modulations, have been fully demonstrated in 2D material-based optical modulators.[19−33] Even though those optical modulators have attracted great interests with large modulation depth and broad operation wavelength range, another figure of merit in an optimum optical modulator, the modulation speed, is rather slow (e.g., ∼1 GHz/MHz for electro-optic modulator/thermo-optic modulator).

All-optical modulation has the potential to circumvent the "electric bottleneck" and gets an ultrafast modulation speed to satisfy the demand of high-speed optical information processing nowadays. The majority of all-optical modulation exploits the optical linearity of graphene-based systems. For example, it has been successfully applied in the linear optical transmittance of graphene-clad microfiber with 38% relative modulation depth and 2.2 ps response time (corresponding to ∼200 GHz).[34,35] In principle, the transient photoexcited nonequilibrium hot carriers will weak the electronic

Received: July 23, 2020
Revised: October 18, 2020
Published: October 28, 2020

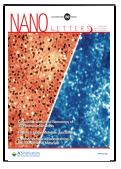

https://dx.doi.org/10.1021/acs.nanolett.0c02972
Nano Lett. 2020, 20, 8053−8058

correlations, block the resonant excitation, and give rise to a highly efficient and an ultrafast modulation of optical nonlinearities with a broad spectrum in graphene. All-optical modulation of nonlinear optical response in graphene has never been explored before. Here, we demonstrate a nonlinear all-optical modulator based on the intrinsic THG of the graphene monolayer. The modulator exhibits excellent performance with a relative modulation depth of more than 90%, the modulation speed of 180 GHz, and a broad operation wavelength range regardless of excitation wavelength.

In this work, graphene monolayer samples were prepared via mechanical exfoliation onto fused silica substrates (Figure 1b).

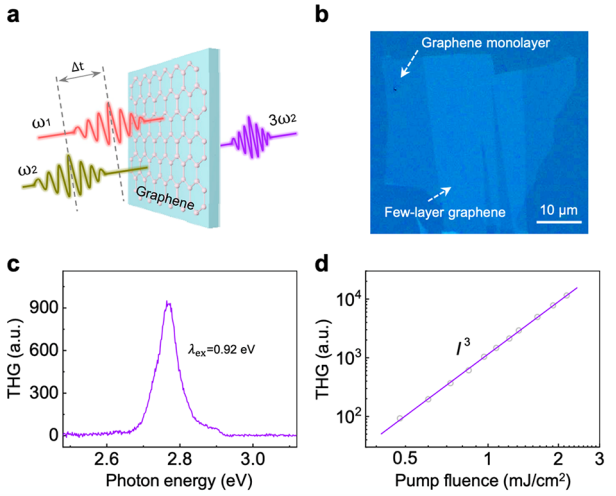

Figure 1. Experimental illustration and intrinsic THG of graphene monolayer. (a) Scheme of pump−probe spectroscopic measurements on the graphene monolayer. Here, ω_1/ω_2 is the pump/probe pulse, and we probe the THG signal of probe pulse at $3\omega_2$. (b) Optical image of the graphene monolayer and few-layer graphene on a fused silica substrate. Scale bars: 10 μm. (c) THG spectrum of graphene monolayer under excitation at 0.92 eV. (d) Power dependence of THG intensity (light gray circle) with curve fitting (purple line) indicating third-order power dependence.

The nonlinear optical response of graphene was investigated in the atmosphere at room temperature with Ti:sapphire oscillator series pumping an optical parametric amplifier (OPA) laser (~150 fs, 250 kHz, 0.78−1.03 eV energy tunable). Under excitation with fundamental frequency ω, the third-order susceptibility $\chi^{3\omega}$ brings about nonlinear polarization $p^{3\omega} = \varepsilon_0\chi^{3\omega}E^{\omega}E^{\omega}E^{\omega}$, where ε_0 is the permittivity of free space and E^{ω} is the incident electric field (Figure 1a).[36,37] As expected, a fundamental femtosecond excitation at $\hbar\omega_2$ = 0.92 eV (under fluence of 0.9 mJ/cm^2) gives rise to the THG centered at $3\hbar\omega_2$ = 2.76 eV (Figure 1c). The nonlinear phenomenon responsible for the upconversion process requires the instantaneous capture of three near-infrared photons to generate a visible photon, hence a cubic dependence of the radiated third harmonic on the intensity of the fundamental is detected in Figure 1d, where a double-logarithm representation is used for clarity.

Under the pulse laser excitation, intraband carrier scattering will bring a broad distribution of nonequilibrium electrons and holes within the first tens of femtoseconds. The temperature of those hot carriers in graphene can reach thousands of Kelvin, much higher than that of the graphene lattice. The hot carriers will then transfer energy to phonons over a characteristic picosecond time scale.[38−40] To investigate how the photoexcited carriers affect the nonlinear optical properties of graphene, we performed time-resolved THG experiments as shown in Figure 2a. After pump pulse ($\hbar\omega_1$ = 3.1 eV, under

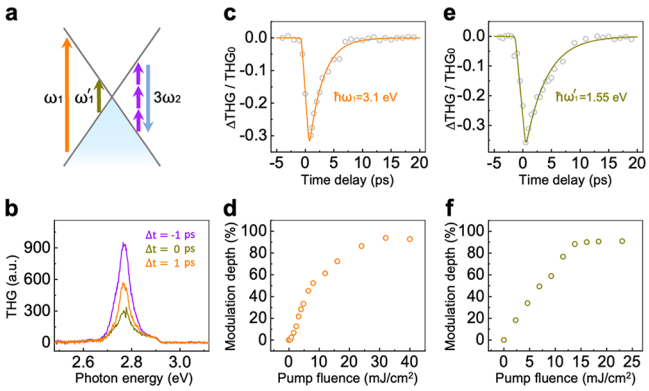

Figure 2. All-optical modulation on THG in graphene monolayer. (a) Scheme describes photoexcited carriers of the pump and probe pulses in the linearly dispersive valence and conduction bands of graphene monolayer. Under the pulse laser excitation ($\hbar\omega_1$ = 3.1 eV or $\hbar\omega_1'$ = 1.55 eV of pump pulse), intraband carrier scattering will bring a broad distribution of nonequilibrium electrons and holes within the first tens of femtoseconds. We investigate how the photoexcited carriers affect the nonlinear optical properties of graphene. (b) THG intensity of graphene monolayer at Δt = −1 ps (purple line), 0 ps (green line), and 1 ps (orange line). With the pump pulse added, the THG of probe pulse is obviously suppressed. (c, e) Time-dependent relative changes in THG of the probe pulse with (c) 3.1 and (e) 1.55 eV pump. In both cases, the ΔTHG/THG$_0$ reaches its minimum intensity within several picoseconds near time zero. (d, f) Fluence-dependent relative modulation depth of the THG intensity with (d) 3.1 and (f) 1.55 eV pump. The relative modulation depth of the graphene monolayer can reach as high as 90%, corresponding to approximately 10 dB.

fluence of 16 mJ/cm^2) with positive time delay being added, the THG intensity of the probe pulse was strongly suppressed (Figure 2b). We defined the relative changes in THG intensity as ΔTHG/THG$_0$ = (THG$_\tau$ − THG$_0$)/THG$_0$, where THG$_\tau$ and THG$_0$ stand for THG intensity of the probe pulse with the pump pulse at time delay τ and without the pump pulse, respectively. The relative changes in THG evolves obviously with time delay between the pump ($\hbar\omega_1$ = 3.1 eV, under a fluence of 4 mJ/cm^2) and probe pulses (under a fluence of 1.6 mJ/cm^2) (Figure 2c). With the time delay increasing, the ΔTHG/THG$_0$ decreases to approximately −0.3 instantly and then rises to zero in the following few picoseconds. Back and forth time-resolved THG values have been measured to exclude the possibility of optical damage in samples caused by the pulse laser (Figure S1). By deconvoluting the time-resolved THG intensity based on laser cross-correlation function, the lifetime obtained from the falling edge of THG intensity with a pump pulse at 3.1 eV is ~2.5 ps. The relative modulation depth, which is defined as the maximum absolute value of ΔTHG/THG around time zero, increases monotonously with increasing pump fluence (Figure 2d).

Upon the femtosecond laser irradiation, electrons in graphene can also be scattered upward along the linear band structure with energy higher than the excitation pulse during thermalization. Therefore, the unique hot carriers in graphene have the chance to enable a broad-spectrum nonlinear modulation regardless of excitation wavelength.[41,42] In order

https://dx.doi.org/10.1021/acs.nanolett.0c02972
Nano Lett. 2020, 20, 8053−8058

to explore the operation wavelength range of our nonlinear all-optical modulator, we also investigated the case of the 1.55 eV pump (under a fluence of 6 mJ/cm^2), where the photon energy is less than the THG of the probe pulse. Similarly, the THG intensity is also suppressed by the prearrived pump pulse (Figure 2e), and a higher pump fluence gives larger suppression (Figure 2f). For both 3.1 and 1.55 eV pump pulses, the relative modulation depth of the graphene monolayer can reach as high as 90%, corresponding to approximately 10 dB. In addition, few-layer graphene and graphite samples show a similar behavior of suppressed THG under the influence of photoexcited carriers (Figure S2).

The dynamic process of time-resolved relative changes in THG is very similar to the carrier dynamics in the graphene monolayer, which has the same rise-up and decay time (Figure S3). Figure 3a illustrates the influence of photoexcited hot carriers on the temporal THG process. At time delay $\Delta t < 0$, the pump pulse is not involved in the THG process and the probe pulse gives a THG spectrum that is the same for the pristine graphene. For $\Delta t > 0$, the hot carriers excited by the pump pulse will occupy the conduction bands, which block the THG transition of the probe pulse. To understand better how the occupied states affect the nonlinear coherent processes and to investigate the relationship between the THG intensity and photocarrier dynamics, we employed real-time TDDFT simulations to quantitatively analyze the time-resolved THG process. These simulations are performed with the homemade time-dependent ab initio package (TDAP),[43] which is based on SIESTA.[44] In our simulations, the vector gauge field $\vec{A}(t) = -c\int_0^t \vec{E}(t')dt'$ is used to photoexcite the crystal. The field strength of the laser pulse $E(t) = E_0\cos(\omega_E t)\exp\left[-\frac{(t-t_0)^2}{2\sigma^2}\right]$ takes the Gaussian shape, where E_0 is the maximum strength of electric field reached at t_0 = 15 fs, $\omega_E = 7.49 \times 10^{14}$ Hz with a 400 nm pump pulse ($\omega_E = 2.22 \times 10^{14}$ Hz with a 1350 nm probe pulse) is the frequency of Gaussian shape light field $E(t)$, and the pulse width 2σ is set as 8 fs (much shorter than the experimental laser pulse width of 100 fs) to simplify the calculations. Consequently, the response time in dynamic simulations is much smaller than that observed in the experiment. The time evolution of the wave functions $\psi_i(\vec{r},t)$ and the time-dependent current are obtained by propagating the Kohn−Sham equations:

$$i\frac{\partial}{\partial t}\psi_i(\vec{r},t) = \left[\frac{1}{2m}\left(\vec{p} - \frac{e}{c}\vec{A}\right)^2 + V(\vec{r},t)\right]\psi_i(\vec{r},t)$$

$$J(t) = \frac{1}{2i}\int_\Omega d\vec{r}\sum_i \{\psi_i^*(\vec{r},t)\nabla\psi_i(\vec{r},t) - \psi_i(\vec{r},t)\nabla\psi_i^*(\vec{r},t)\}$$

Through Fourier transform of the time-dependent current, the time-resolved HHG spectrum is obtained:

$$\mathrm{HHG}(\omega) = \left|\int_0^\tau \omega^2 J(t)\exp(-i\omega t)dt\right|^2$$

Here, ω is the frequency of energy in HHG spectrum. Figure 3b shows the relative changes in time-resolved THG from our first-principles dynamic simulations, where the hot carriers obviously bring a suppression in THG. Note that in these simulations we fixed the ions in graphene cells without considering the scattering between electrons and phonons, which might result in a faster relaxation time as obtained from the falling edge of THG intensity than the experimental results. Both experiments and simulations indicate that THG intensity decreases monotonously with increasing pump fluence, even across the optical gain regime with the inverted Dirac Fermion population (Figure 3c).[45] However, the coherent THG process could not be fully turned off, and the graphene monolayer still holds 10% THG intensity under the blocking of resonant excitation. The proportion of photoexcited electrons in energy bands with various time delay and pump fluence have been illustrated for comparison (Figure S4). We also performed theoretical calculations on all-optical modulation of THG in a graphene monolayer with the 1.55 eV pump, and the calculated time-resolved relative changes in THG intensity and variations in THG intensity with the pump fluence show the same tendency (Figure S5).

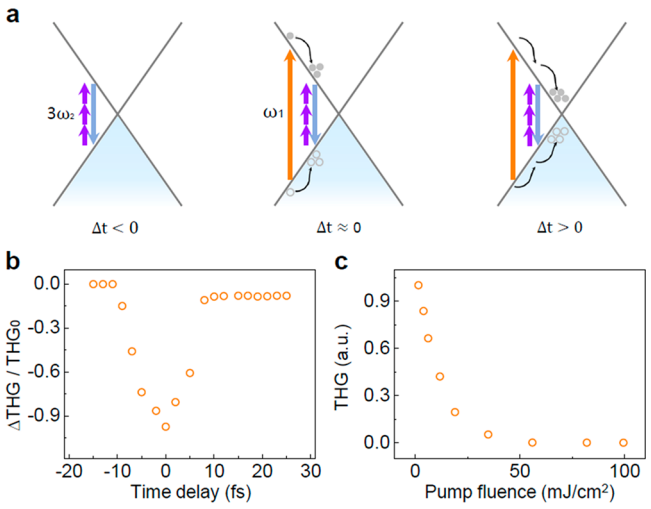

Figure 3. Theoretical simulations of all-optical modulation on THG from a graphene monolayer with a 3.1 eV pump. (a) Schematic representation of the ultrafast temporal dynamics of photoexcited carriers in graphene. At the time delay $\Delta t < 0$, the pump pulse is not involved in the THG process and the probe pulse gives a THG spectrum that is the same for the pristine graphene, whereas for $\Delta t > 0$, the carriers excited by a pump pulse will occupy the transition states of THG of the probe pulse. The simulative pulse width is 2σ = 8 fs for clarity. (b) Evolution of the relative change in THG intensity from the graphene monolayer under different time delays between the 3.1 eV pump and the 0.92 eV probe. (c) Simulative THG intensity variation with different pump fluence. Obviously, the THG intensity decreases monotonously with increasing pump fluence.

The modulation of optical harmonic generation by optical pump can be potentially applied to other 2D materials, such as the MoS_2 monolayer. Different with graphene with a centrosymmetric crystal structure, the MoS_2 monolayer has both odd and even order nonlinear optical response. We use a pulse laser with a photon energy of 3.1 eV (under a fluence of 11 mJ/cm^2) to pump the MoS_2 monolayer, where the light intensity is attenuated to avoid strong intrinsic photoluminescence. Another pulse at 0.92 (under a fluence of 0.5 mJ/cm^2) or 0.62 eV (under a fluence of 0.6 mJ/cm^2) is used as the probe pulse to excite SHG or THG of MoS_2 monolayer with the emission energy around the bandgap (Figure 4a). As shown in Figure 4b, c, the SHG and THG of MoS_2 monolayer are also significantly suppressed when the pump pulse is present, with a relaxation time of ∼12 ps for both situations (corresponding to 40 GHz). These dynamic processes of

https://dx.doi.org/10.1021/acs.nanolett.0c02972
Nano Lett. 2020, 20, 8053−8058

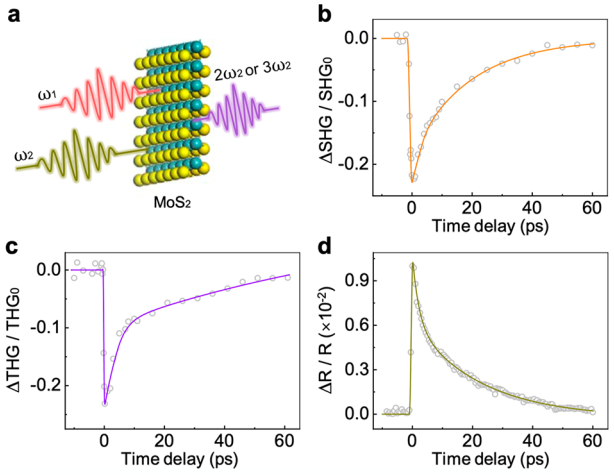

Figure 4. All-optical modulation on SHG and THG from MoS_2monolayer with 3.1 eV pump. (a) Scheme of pump−probe spectroscopic measurements on MoS_2 monolayer. Here, ω_1/ω_2 is the pump/probe pulse, and we probe the SHG/THG signal of the probe pulse at $2\omega_2/3\omega_2$. (b, c) Time-dependent relative change in SHG and THG intensity with the 0.92 and 0.62 eV probe. With the pump pulse added, the SHG and THG of MoS_2 monolayer are also suppressed with the relaxation time of ∼12 ps for both situations. (d) Evolution of transient absorption signal of MoS_2 monolayer with the 3.1 eV pump and 1.8 eV probe, which is consistent with optical harmonic generation dynamic processes.

optical harmonic generation are also consistent with the transient absorption measurements of the MoS_2 monolayer with 3.1 eV (under a fluence of 2.3 mJ/cm^2) pump and 1.8 eV probe (under a fluence of 0.07 mJ/cm^2) (Figure 4d), whereas the modulation depth of MoS_2 is only 16% (43%) for the SHG (THG) process, much smaller than that of the graphene monolayer (Figure S6).

In summary, we have demonstrated an efficient route to engineer the optical harmonic generation of 2D materials by the ultrafast optical pump. Particularly, the pump-induced photoexcited carriers enable graphene-based all-optical modulator ultrafast modulation speed, ultrahigh modulation depth, and broad operation wavelength range, paving the way for optically tunable modulators for applications in optical communication and information processing. The real-time TDDFT simulations unveil that the nonlinear dynamics of the photoexcited carriers account for the suppressing of coherent nonlinear process in graphene. In general, the modulation of optical harmonic generation can enable enormous future design toward on-chip all-optical devices with novel functionalities.

METHODS

Graphene and MoS_2 Sample Preparation for Optical Measurements. The graphene monolayer was prepared via mechanical exfoliation from bulk graphite onto fused silica substrates. MoS_2 monolayer samples were grown on a fused silica substrate with a thickness of 0.5 mm by a NaCl-assisted CVD method using MoO_3 and S powders as precursors. Ten milligrams of MoO_3 (99%, Sigma-Aldrich) powder and 2 mg of NaCl (Greagent, 99.95%) were mixed and placed at the center of tube furnace and 1 g of sulfur (99%, Sigma-Aldrich) powder was placed upstream of a quartz tube. The fused silica was placed downstream 10 cm away from the Mo source. The chamber of the furnace was then flushed with argon for an inert atmosphere and subsequently ramped up to the optimized growth temperature (∼780 °C) with 100 sccm argon. During growth, the temperature for sulfur evaporation was ∼120 °C. The entire process was carried out under ∼150 Pa and the growth duration was set as 15 min. After the growth, the system was naturally cooled to room temperature. We measured the Raman spectra using self-bulit equipment with a 532 nm CW laser to ensure the graphene and MoS_2 samples are monolayers (Figure S7a, b).

Fabrication and Electrical Measurement of the Graphene Monolayer Back-Gate FET (Field-Effect Transistor). The graphene monolayer were exfoliated from bulk graphite onto Si/SiO_2 substrates (280 nm thick SiO_2). Subsequently, the metal electrodes of the source and drain were fabricated by photolithography, electron-beam thermal evaporation of Ti/Au (10 nm/50 nm), and lift-off processes. In this graphene back-gate FET, the 280 nm SiO_2 served as the back-gate dielectric layer. The electrical characteristics of the graphene monolayer back-gate FET were measured at room temperature using a Keithley 4200 semiconductor characterization system (Keithely 4200 SCS) in a dark environment (Figure S7c, d).

Transient Absorption Spectrum. The pump−probe measurements were performed with femtosecond pulses (Spectra-Physics Mai Tai laser, ∼100 fs, 80 MHz) generated by a Ti:sapphire oscillator and an optical parametric oscillator (OPO). The transient absorption signal, defined as $\Delta R/R = (R_{\text{with pump}} - R_{\text{without pump}})/R_{\text{without pump}}$, was recorded by a PMT and a lock-in amplifier with reflective geometry. The diameters of the focused pump and probe pulses were ∼0.6 and 0.8 μm, respectively.

Time-Resolved THG and SHG. The time-resolved THG and SHG were excited with femtosecond pulses (Coherent laser, ∼150 fs, 250 kHz) generated by a Ti:sapphire oscillator series pumping an OPA. To investigate the evolution of THG intensity of graphene monolayer, we pumped graphene at 3.1 or 1.55 eV and probed the THG intensity at 0.92 eV (under a fluence of 1.6 mJ/cm^2). We collected the THG signal by a 425 nm long-pass filter (650 nm short-pass filter for 1.55 eV pump) with a spectrometer equipped with a liquid-nitrogen-cooled silicon charged coupled device (CCD). For the time-resolved SHG and THG measurements of MoS_2 monolayer, we pumped MoS_2 at 3.1 eV (under a fluence of 11 mJ/cm^2) and probed the SHG intensity at 0.92 eV (under a fluence of 0.5 mJ/cm^2) and the THG intensity at 0.62 eV (under a fluence of 0.6 mJ/cm^2). More details about our experimental setup can be found in Figure S8.

TDDFT Simulations. The simulations were performed using a homemade real-time TDDFT code. The graphene monolayer was simulated with a unit cell of two atoms. An auxiliary real-space grid equivalent to a plane-wave cutoff of 250 Ry was used, using the Gamma centered k-mesh of 24 × 24 × 1 to sample the Brillouin zone. The exchange-correlation function was described by Troullier−Martins pseudopotentials,[46] in the adiabatic local density approximation (LDA).[47] The time step for the wave function evolution was 20 attoseconds for both electrons and ions.

ASSOCIATED CONTENT

Supporting Information

The Supporting Information is available free of charge at https://pubs.acs.org/doi/10.1021/acs.nanolett.0c02972.

https://dx.doi.org/10.1021/acs.nanolett.0c02972
Nano Lett. 2020, 20, 8053−8058

Reversible all-optical modulation on harmonic generation of MoS_2 and graphene monolayer; comparisons between THG response with all-optical modulation of graphite, few-layer graphene, and graphene monolayer; transient absorption signal of graphene monolayer; theory simulations of probe excited electrons with various time-delay and pump fluence; theoretical simulations of all-optical modulation on THG from graphene monolayer with 1.55 eV pump; fluence dependence of the SHG and THG intensity of MoS_2 monolayer with 3.1 eV pump; Raman spectra of graphene and MoS_2 monolayer; scheme of the optical pump−probe measurements setup (PDF)

AUTHOR INFORMATION

Corresponding Author

Kaihui Liu − *State Key Laboratory for Mesoscopic Physics, Academy for Advanced Interdisciplinary Studies, School of Physics and International Center for Quantum Materials, Collaborative Innovation Center of Quantum Matter, Peking University, Beijing 100871, China;* orcid.org/0000-0002-8781-2495; Email: khliu@pku.edu.cn

Authors

Yang Cheng − *State Key Laboratory for Mesoscopic Physics, Academy for Advanced Interdisciplinary Studies, School of Physics, Peking University, Beijing 100871, China;* orcid.org/0000-0003-2925-8606

Hao Hong − *State Key Laboratory for Mesoscopic Physics, Academy for Advanced Interdisciplinary Studies, School of Physics, Peking University, Beijing 100871, China*

Hui Zhao − *Institute of Physics, Chinese Academy of Sciences, Beijing 100190, China*

Chunchun Wu − *State Key Laboratory for Mesoscopic Physics, Academy for Advanced Interdisciplinary Studies, School of Physics, Peking University, Beijing 100871, China; State Key Laboratory of Electronic Thin Films and Integrated Devices, University of Electronic Science and Technology of China, Chengdu 610054, China*

Yu Pan − *State Key Laboratory for Mesoscopic Physics, Academy for Advanced Interdisciplinary Studies, School of Physics, Peking University, Beijing 100871, China*

Can Liu − *State Key Laboratory for Mesoscopic Physics, Academy for Advanced Interdisciplinary Studies, School of Physics, Peking University, Beijing 100871, China; Physical Science Laboratory, Huairou National Comprehensive Science Center, Beijing 101400, China;* orcid.org/0000-0001-5451-4144

Yonggang Zuo − *State Key Laboratory for Mesoscopic Physics, Academy for Advanced Interdisciplinary Studies, School of Physics, Peking University, Beijing 100871, China; Institute of Physics, Chinese Academy of Sciences, Beijing 100190, China*

Zhihong Zhang − *International Center for Quantum Materials, Collaborative Innovation Center of Quantum Matter, Peking University, Beijing 100871, China; Physical Science Laboratory, Huairou National Comprehensive Science Center, Beijing 101400, China*

Jin Xie − *State Key Laboratory for Mesoscopic Physics, Academy for Advanced Interdisciplinary Studies, School of Physics, Peking University, Beijing 100871, China*

Jinhuan Wang − *State Key Laboratory for Mesoscopic Physics, Academy for Advanced Interdisciplinary Studies, School of Physics, Peking University, Beijing 100871, China*

Dapeng Yu − *Shenzhen Institute for Quantum Science and Engineering and Department of Physics, Southern University of Science and Technology, Shenzhen 518055, China*

Yu Ye − *State Key Laboratory for Mesoscopic Physics, Academy for Advanced Interdisciplinary Studies, School of Physics, Peking University, Beijing 100871, China;* orcid.org/0000-0001-6046-063X

Sheng Meng − *Institute of Physics, Chinese Academy of Sciences, Beijing 100190, China;* orcid.org/0000-0002-1553-1432

Complete contact information is available at: https://pubs.acs.org/10.1021/acs.nanolett.0c02972

Author Contributions

†Y.C., H.H., and H.Z. contributed equally to this work. K.L. conceived of the project. C.W. and Z.Z. provided the graphene sample. Y.Z. and J.W. provided the MoS_2 sample. Y.C., H.H., and J.X. performed the time-dependent THG and SHG intensity measurements. H.Z. calculated the carrier dynamics of graphene using real-time TDDFT. Y.P. and Y.Y. performed the electrical measurements of graphene monolayer back-gate FET. C.L., D.Y., S.M., and K.L. analyzed and discussed the data.

Notes

The authors declare no competing financial interest.

ACKNOWLEDGMENTS

This work is supported by Beijing Natural Science Foundation (JQ19004), Beijing Excellent Talents Training Support (2017000026833ZK11), the National Natural Science Foundation of China (51991340 and 51991342), the National Key R&D Program of China (2016YFA0300903 and 2016YFA0300804), the Key R&D Program of Guangdong Province (2020B010189001, 2019B010931001, 2018B010109009, and 2018B030327001), Beijing Municipal Science & Technology Commission (Z191100007219005), Beijing Graphene Innovation Program (Z181100004818003), Bureau of Industry and Information Technology of Shenzhen (Graphene platform 201901161512), Guangdong Innovative and Entrepreneurial Research Team Program (2016ZT06D348), and the Science, Technology and Innovation Commission of Shenzhen Municipality (KYTDPT20181011104202253).

REFERENCES

(1) Bonaccorso, F.; Sun, Z.; Hasan, T.; Ferrari, A. Graphene photonics and optoelectronics. *Nat. Photonics* **2010**, *4*, 611−622.

(2) Avouris, P. Graphene: electronic and photonic properties and devices. *Nano Lett.* **2010**, *10*, 4285−4294.

(3) Novoselov, K. S.; Fal'ko, V. I.; Colombo, L.; Gellert, P. R.; Schwab, M. G.; Kim, K.; et al. A roadmap for graphene. *Nature* **2012**, *490*, 192−200.

(4) Koppens, F. H.; Chang, D. E.; Garcia de Abajo, F. J. Graphene plasmonics: a platform for strong light−matter interactions. *Nano Lett.* **2011**, *11*, 3370−3377.

(5) Nair, R. R.; Blake, P.; Grigorenko, A. N.; Novoselov, K. S.; Booth, T. J.; et al. Fine structure constant defines visual transparency of graphene. *Science* **2008**, *320*, 1308−1308.

(6) Mak, K. F.; Sfeir, M. Y.; Wu, Y.; Lui, C. H.; Misewich, J. A.; et al. Measurement of the optical conductivity of graphene. *Phys. Rev. Lett.* **2008**, *101*, 196405.

(7) Boyd, R. W., Prato, D. *Nonlinear Optics*, 2 nd ed.; Elsevier Science: New York, 2008.

(8) Reshef, O.; Giese, E.; Zahirul Alam, M.; De Leon, I.; Upham, J.; et al. Beyond the perturbative description of the nonlinear optical response of low-index materials. *Opt. Lett.* **2017**, *42*, 3225−3228.
(9) Reyna, A. S.; de Araújo, C. B. High-order optical nonlinearities in plasmonic nanocomposites—a review. *Adv. Opt. Photonics* **2017**, *9*, 720−774.
(10) Bao, Q.; Zhang, H.; Wang, Y.; Ni, Z.; Yan, Y.; et al. Atomic layer graphene as a saturable absorber for ultrafast pulsed lasers. *Adv. Funct. Mater.* **2009**, *19*, 3077−3083.
(11) Sun, Z.; Hasan, T.; Torrisi, F.; Popa, D.; Privitera, G.; et al. Graphene mode-locked ultrafast laser. *ACS Nano* **2010**, *4*, 803−810.
(12) Gu, T.; Petrone, N.; McMillan, J. F.; van der Zande, A.; Yu, M.; et al. Regenerative oscillation and four-wave mixing in graphene optoelectronics. *Nat. Photonics* **2012**, *6*, 554−559.
(13) Peres, N.; Bludov, Y. V.; Santos, J. E.; Jauho, A.-P.; Vasilevskiy, M. Optical bistability of graphene in the terahertz range. *Phys. Rev. B: Condens. Matter Mater. Phys.* **2014**, *90*, 125425.
(14) Yoshikawa, N.; Tamaya, T.; Tanaka, K. High-harmonic generation in graphene enhanced by elliptically polarized light excitation. *Science* **2017**, *356*, 736−738.
(15) Cox, J. D.; Marini, A.; de Abajo, F. J. Plasmon-assisted high-harmonic generation in graphene. *Nat. Commun.* **2017**, *8*, 14380.
(16) Hafez, H. A.; Kovalev, S.; Deinert, J. C.; Mics, Z.; Green, B.; et al. Extremely efficient terahertz high-harmonic generation in graphene by hot Dirac fermions. *Nature* **2018**, *561*, 507−511.
(17) Cheng, B.; Kanda, N.; Ikeda, T. N.; Matsuda, T.; Xia, P.; et al. Efficient Terahertz Harmonic Generation with Coherent Acceleration of Electrons in the Dirac Semimetal Cd3As2. *Phys. Rev. Lett.* **2020**, *124*, 117402.
(18) Kovalev, S.; Dantas, R. M. A.; Germanskiy, S.; Deinert, J.-C.; Green, B.; Ilyakov, I.; Awari, N.; Chen, M.; Bawatna, M.; Ling, J.; et al. Non-perturbative terahertz high-harmonic generation in the three-dimensional Dirac semimetal Cd3As2. *Nat. Commun.* **2020**, *11*, 2451.
(19) Thalmeier, P.; Dóra, B.; Ziegler, K. Surface acoustic wave propagation in graphene. *Phys. Rev. B: Condens. Matter Mater. Phys.* **2010**, *81*, 041409.
(20) Yan, H.; Li, Z.; Li, X.; Zhu, W.; Avouris, P.; et al. Infrared spectroscopy of tunable Dirac terahertz magneto-plasmons in graphene. *Nano Lett.* **2012**, *12*, 3766−3771.
(21) Crassee, I.; Orlita, M.; Potemski, M.; Walter, A. L.; Ostler, M.; et al. Intrinsic terahertz plasmons and magnetoplasmons in large scale monolayer graphene. *Nano Lett.* **2012**, *12*, 2470−2474.
(22) Kim, J. T.; Chung, K. H.; Choi, C. G. Thermo-optic mode extinction modulator based on graphene plasmonic waveguide. *Opt. Express* **2013**, *21*, 15280−15286.
(23) Shimano, R.; Yumoto, G.; Yoo, J. Y.; Matsunaga, R.; Tanabe, S.; Hibino, H.; Morimoto, T.; Aoki, H.; et al. Quantum Faraday and Kerr rotations in graphene. *Nat. Commun.* **2013**, *4*, 1841.
(24) Farhat, M.; Guenneau, S.; Bağcı, H. Exciting graphene surface plasmon polaritons through light and sound interplay. *Phys. Rev. Lett.* **2013**, *111*, 237404.
(25) Gan, S.; Cheng, C.; Zhan, Y.; Huang, B.; Gan, X.; et al. A highly efficient thermo-optic microring modulator assisted by graphene. *Nanoscale* **2015**, *7*, 20249−20255.
(26) Sun, Z. P.; Martinez, A.; Wang, F. Optical modulators with 2D layered materials. *Nat. Photonics* **2016**, *10*, 227−238.
(27) Lin, H.; Song, Y.; Huang, Y.; Kita, D.; Deckoff-Jones, S.; et al. Chalcogenide glass-on-graphene photonics. *Nat. Photonics* **2017**, *11*, 798−805.
(28) Jiang, T.; Huang, D.; Cheng, J. L.; Fan, X. D.; Zhang, Z. H.; et al. Gate-tunable third-order nonlinear optical response of massless Dirac fermions in graphene. *Nat. Photonics* **2018**, *12*, 430−436.
(29) Soavi, G.; Wang, G.; Rostami, H.; Purdie, D. G.; De Fazio, D.; et al. Broadband, electrically tunable third-harmonic generation in graphene. *Nat. Nanotechnol.* **2018**, *13*, 583−588.
(30) Chen, K.; Zhou, X.; Cheng, X.; Qiao, R.; Cheng, Y.; et al. Graphene photonic crystal fibre with strong and tunable light−matter interaction. *Nat. Photonics* **2019**, *13*, 754−759.
(31) Wang, B.; Blaize, S.; Seok, J.; Kim, S.; Yang, H.; et al. Plasmonic-based subwavelength graphene-on-hBN modulator on silicon photonics. *IEEE J. Sel. Top. Quantum Electron.* **2019**, *25*, 1−6.
(32) Shinokita, K.; Wang, X.; Miyauchi, Y.; Watanabe, K.; Taniguchi, T.; et al. Continuous control and enhancement of excitonic valley polarization in monolayer WSe2 by electrostatic doping. *Adv. Funct. Mater.* **2019**, *29*, 1900260.
(33) Lee, I.-H.; Yoo, D.; Avouris, P.; Low, T.; Oh, S.-H. Graphene acoustic plasmon resonator for ultrasensitive infrared spectroscopy. *Nat. Nanotechnol.* **2019**, *14*, 313−319.
(34) Siegman, A. E. *Lasers*; University Science Books, Mill Valley, CA, 1986.
(35) Li, W.; Chen, B. G.; Meng, C.; Fang, W.; Xiao, Y.; et al. Ultrafast All-Optical Graphene Modulator. *Nano Lett.* **2014**, *14*, 955−959.
(36) Kumar, N.; Kumar, J.; Gerstenkorn, C.; Wang, R.; Chiu, H.-Y.; et al. Third harmonic generation in graphene and few-layer graphite films. *Phys. Rev. B: Condens. Matter Mater. Phys.* **2013**, *87*, 121406.
(37) Hong, S.-Y.; Dadap, J. I.; Petrone, N.; Yeh, P.-C.; Hone, J.; et al. Optical third-harmonic generation in graphene. *Phys. Rev. X* **2013**, *3*, 021014.
(38) Huang, L.; Hartland, G. V.; Chu, L.-Q.; Feenstra, R. M.; Lian, C.; et al. Ultrafast transient absorption microscopy studies of carrier dynamics in epitaxial graphene. *Nano Lett.* **2010**, *10*, 1308−1313.
(39) Tielrooij, K.; Song, J.; Jensen, S. A.; Centeno, A.; Pesquera, A.; et al. Photoexcitation cascade and multiple hot-carrier generation in graphene. *Nat. Phys.* **2013**, *9*, 248−252.
(40) Tielrooij, K.-J.; Piatkowski, L.; Massicotte, M.; Woessner, A.; Ma, Q.; et al. Generation of photovoltage in graphene on a femtosecond timescale through efficient carrier heating. *Nat. Nanotechnol.* **2015**, *10*, 437−443.
(41) Liu, W.-T.; Wu, S.; Schuck, P.; Salmeron, M.; Shen, Y.; et al. Nonlinear broadband photoluminescence of graphene induced by femtosecond laser irradiation. *Phys. Rev. B: Condens. Matter Mater. Phys.* **2010**, *82*, 081408.
(42) Zhuo, S.; Shao, M.; Lee, S.-T. Upconversion and down-conversion fluorescent graphene quantum dots: ultrasonic preparation and photocatalysis. *ACS Nano* **2012**, *6*, 1059−1064.
(43) Lian, C.; Hu, S.-Q.; Guan, M.-X.; Meng, S. Momentum-resolved TDDFT algorithm in atomic basis for real time tracking of electronic excitation. *J. Chem. Phys.* **2018**, *149*, 154104.
(44) Soler, J. M.; Artacho, E.; Gale, J. D.; García, A.; Junquera, J.; et al. The SIESTA method for ab initio order-N materials simulation. *J. Phys.: Condens. Matter* **2002**, *14*, 2745.
(45) Li, T.; Luo, L.; Hupalo, M.; Zhang, J.; Tringides, M.; et al. Femtosecond population inversion and stimulated emission of dense Dirac fermions in graphene. *Phys. Rev. Lett.* **2012**, *108*, 167401.
(46) Troullier, N.; Martins, J. L. Efficient pseudopotentials for plane-wave calculations. *Phys. Rev. B: Condens. Matter Mater. Phys.* **1991**, *43*, 1993.
(47) Perdew, J. P.; Zunger, A. Self-consistent equations including exchange and correlation effects. *Phys. Rev. B: Condens. Matter Mater. Phys.* **1981**, *23*, 5048−5079.

https://dx.doi.org/10.1021/acs.nanolett.0c02972
Nano Lett. 2020, 20, 8053−8058